

# Swift $GW$ beyond 10,000 electrons using fractured stochastic orbitals

Vojtěch Vlček,<sup>1,2,\*</sup> Wenfei Li,<sup>1,†</sup> Roi Baer,<sup>3,‡</sup> Eran Rabani,<sup>4,5,§</sup> and Daniel Neuhauser<sup>1,¶</sup>

<sup>1</sup>*Department of Chemistry and Biochemistry, University of California, Los Angeles California 90095, USA*

<sup>2</sup>*After July 1 2018: Department of Chemistry and Biochemistry,  
University of California, Santa Barbara California 93106, USA*

<sup>3</sup>*Fritz Haber Center for Molecular Dynamics, Institute of Chemistry,  
The Hebrew University of Jerusalem, Jerusalem 91904, Israel*

<sup>4</sup>*Department of Chemistry, University of California and Materials Science Division,  
Lawrence Berkeley National Laboratory, Berkeley, California 94720, USA*

<sup>5</sup>*The Raymond and Beverly Sackler Center for Computational Molecular  
and Materials Science, Tel Aviv University, Tel Aviv, Israel 69978*

(Dated: May 29, 2018)

We introduce the concept of fractured stochastic orbitals (FSOs), short vectors that sample a small number of space points and enable an efficient stochastic sampling of any general function. As a first demonstration, FSOs are applied in conjunction with simple direct-projection to accelerate our recent stochastic  $GW$  technique; the new developments enable accurate prediction of  $G_0W_0$  quasiparticle energies and gaps for systems with up to  $N_e > 10,000$  electrons, with small statistical errors of  $\pm 0.05$  eV and using less than 2000 core CPU hours. Overall, stochastic  $GW$  scales now linearly (and often sub-linearly) with  $N_e$ .

## I. INTRODUCTION

Fundamental band gaps and quasiparticle (QP) energies determine the electronic properties of molecules and solids, but their first principles calculations are nontrivial. Density functional theory (DFT) [1] is usually used for ground state charge densities and atomic geometries, but gives wrong QP energies.[2–4] Going beyond DFT is computationally demanding. For small molecules, configuration interaction [5–7] and the equation of motion coupled cluster technique [8–10] yield accurate QP energies, but scale very steeply with the number of electrons.

In recent years, the  $GW$  approximation [4, 7, 11] became the predominant framework for QP calculations. The method describes all many-body effects through the single-particle self-energy, approximated as  $\Sigma = GW$ , where  $G$  is the single particle Green’s function and  $W$  is the screened Coulomb interaction.  $GW$  provides accurate ionization energies and electron affinities for both molecules and solids, at a steep scaling.[12–18] Most computational improvements focus on reducing the prefactor rather than lowering the overall scaling.[14, 17]

We recently introduced a stochastic formulation of  $GW$  [19] that expresses the self-energy as a statistical quantity, averaged over random samplings. The resulting stochastic  $GW$  method reproduces the results of deterministic  $GW$  [20] but is very fast so it is applicable to large systems with thousands of valence electrons.[19, 21, 22]

Here, two major improvements of stochastic  $GW$  are introduced, and together they enable routine calculations of QP energies for systems with  $N_e > 10,000$ . The first relates to the projection of random functions to the occupied subspace. Originally, we used a Chebyshev projection that is quite expensive. Here, we use a simpler direct projection method that formally scales as  $O(N_e^2)$  but with a small prefactor so it significantly reduces the overall effort (as long as the occupied eigenstates or their linear combinations are available).

The second improvement relates to the conversion of causal potentials to time-ordered potentials, which is a necessary ingredient in stochastic  $GW$ . Originally, we used for this a stochastic basis (stochastic resolution of the identity, S-RI), but it turns out that the required number of stochastic basis functions grows with system size, destroying the overall linear scaling for large systems. To circumvent this, we develop a new approach based on short stochastic vectors, which we label as fractured stochastic resolution of the identity (FS-RI); the method does not lower the accuracy but is much cheaper, thereby enabling the treatment of very large systems with  $N_e > 10,000$ . FS-RI has potentially a large number of applications, and we use stochastic  $GW$  here to demonstrate its efficiency.

With direct projection and FS-RI, stochastic  $GW$  is efficient and scales very gently, as demonstrated here for finite molecules (acenes and  $C_{60}$  molecules) and periodic systems with large supercells.

The paper is organized as follows: Deterministic  $GW$  is reviewed in Sec. II. In Sec. III we briefly explain (see Refs. 19 and 20 for details) how the stochastic expansion of  $G$  converts  $GW$  into the action of  $W$  on a source term. Sec. IV reviews the use of linear response with deterministic or stochastic TDH (time-dependent Hartree) for acting with  $W^R$ , the causal (retarded) effective interaction. In Sec. V fractured orbitals are introduced

\* vojtech.vlcek@gmail.com

† liwenfei@chem.ucla.edu

‡ roi.baer@huji.ac.il

§ eran.rabani@berkeley.edu

¶ dxn@ucla.edu

and used to convert the application of  $W^R$  to  $W$ , and the overall algorithm is reviewed in Sec. VI. Results for molecules and solids are shown in Sec. VII, followed by conclusions in Sec. VIII.

## II. THE GW METHOD

We first outline deterministic *GW*. The starting point is a specific real-valued KS (Kohn-Sham) orbital  $\phi$  (typically the HOMO or LUMO) and associated eigenvalue  $\varepsilon^{KS}$  that fulfill  $H_0\phi = \varepsilon^{KS}\phi$ . Here the KS-DFT Hamiltonian is (using atomic units, and treating closed-shell systems):

$$H_0 = -\frac{1}{2}\nabla^2 + v_{\text{nuc}}[n_0] + v_{\text{H}}[n_0] + v_{\text{xc}}[n_0],$$

and we introduced the ground state density ( $n_0(\mathbf{r})$ ) and the nuclear and exchange-correlation potentials, while the Hartree potential is  $v_{\text{H}}[n](\mathbf{r}) = \int \nu(\mathbf{r}, \mathbf{r}') n(\mathbf{r}') d\mathbf{r}'$  with  $\nu(\mathbf{r}, \mathbf{r}') = |\mathbf{r} - \mathbf{r}'|^{-1}$ . In the diagonal approximation, the associated QP energy fulfills:[4]

$$\varepsilon^{QP} = \varepsilon^{KS} + \langle \phi | X + \Sigma(\omega = \varepsilon^{QP}) - v_{\text{xc}} | \phi \rangle, \quad (1)$$

where  $X$  is the Fock exchange-operator and  $\Sigma$  refers throughout to the polarization self-energy (rather than the full one).

The frequency-resolved matrix element of the polarization self energy is obtained from the time-dependent form,  $\langle \phi | \Sigma(\omega) | \phi \rangle \equiv \int \langle \phi | \Sigma(t) | \phi \rangle e^{-\frac{1}{2}\gamma^2 t^2} e^{i\omega t} dt$  where  $\gamma$  is an energy broadening term for converging the time integration.[23] The required polarization self-energy  $\Sigma(t)$  has a very simple direct product form in the *GW* approximation:[4]

$$\Sigma(\mathbf{r}, \mathbf{r}', t) = iG(\mathbf{r}, \mathbf{r}', t)W(\mathbf{r}, \mathbf{r}', t), \quad (2)$$

where  $G$  is the Green's function (detailed below), and  $W$  the effective polarization interaction. We use here the one-shot  $G_0W_0$  approximation, but omit the 0 subscript throughout, as well as the  $P$  (polarization) subscript on  $\Sigma$  and  $W$ . Despite its elegance, it is expensive to directly calculate  $\langle \phi | \Sigma(t) | \phi \rangle$  using Eq. (2) and the first goal of stochastic *GW* is to convert the direct product to an initial value expression as detailed below.

## III. STOCHASTIC PARADIGM FOR RESOLVING G

### A. Resolution of identity

Our starting point is a set of random functions on a grid, each labeled  $\bar{\zeta}(\mathbf{r})$ . The simplest choice is real discrete stochastic functions that have a random sign at each point:

$$\bar{\zeta}(\mathbf{r}) = \pm(dV)^{-\frac{1}{2}}$$

( $dV$  is the grid volume element). The stochastic functions fulfill  $\{\bar{\zeta}(\mathbf{r})\bar{\zeta}(\mathbf{r}')\} = (dV)^{-1}\delta_{\mathbf{r},\mathbf{r}'}$ , where  $\delta_{\mathbf{r},\mathbf{r}'}$  is a Kronecker delta and the  $\{\dots\}$  refers to a statistical average over all stochastic functions. This implies a resolution of the identity relation,  $\mathcal{I} = \{|\bar{\zeta}\rangle\langle\bar{\zeta}|\}$ . In practice we need to use a finite number (labeled  $N_{\bar{\zeta}}$ ) of stochastic functions and the resolution becomes approximate

$$\mathcal{I} \simeq \frac{1}{N_{\bar{\zeta}}} \sum_{\bar{\zeta}} |\bar{\zeta}\rangle\langle\bar{\zeta}|. \quad (3)$$

### B. Separable expression for the Green's function

It is easy to show that the Kohn-Sham Green's function is given by the operator form  $iG(t) = e^{-iH_0t}((\mathcal{I} - \mathcal{P})\theta(t) - \mathcal{P}\theta(-t))$  where the projection operator to the  $N_{\text{occ}}$  occupied states is  $\mathcal{P} = \sum_{n \leq N_{\text{occ}}} |\phi_n\rangle\langle\phi_n|$ . To make a separable form, multiply  $iG(t)$  by Eq. (3), leading to:

$$iG(\mathbf{r}, \mathbf{r}', t) \simeq \frac{1}{N_{\bar{\zeta}}} \sum_{\bar{\zeta}} \zeta(\mathbf{r}, t)\bar{\zeta}(\mathbf{r}'), \quad (4)$$

where  $|\zeta(t)\rangle \equiv iG(t)|\bar{\zeta}\rangle$ . Eq. (4) is the main ingredient of stochastic *GW*, reformulating the Green's function as a sum over separable terms.

To evaluate  $|\zeta(t)\rangle$ , start with the negative-time Green's function which is a propagator of the occupied states,  $iG(t < 0) = -e^{-iH_0t}\mathcal{P}$ , so:

$$|\zeta(t < 0)\rangle = -e^{-iH_0t}|\zeta^v\rangle, \quad (5)$$

where we define a stochastic occupied (valence) state  $|\zeta^v\rangle = \mathcal{P}|\bar{\zeta}\rangle$ . Similarly for positive times the Green's function is the propagator of unoccupied (conduction) states,  $iG(t > 0) = e^{-iH_0t}(\mathcal{I} - \mathcal{P})$ , so:

$$|\zeta(t > 0)\rangle = e^{-iH_0t}|\zeta^c\rangle, \quad (6)$$

where  $|\zeta^c\rangle = (\mathcal{I} - \mathcal{P})|\bar{\zeta}\rangle = |\bar{\zeta}\rangle - \zeta^v$ .

### C. Projective Filtering

The next stage is therefore to calculate  $\mathcal{P}|\bar{\zeta}\rangle$ . Previously we used Chebyshev filtering which scales linearly with system size, but with a large prefactor. Therefore as long as the occupied states are available (i.e., for systems with up to tens of thousands of electrons) it is faster to use projective filtering, i.e.,

$$\zeta^v(\mathbf{r}) = \langle \mathbf{r} | \mathcal{P} \bar{\zeta} \rangle = \sum_{n \leq N_{\text{occ}}} \phi_n(\mathbf{r}) \langle \phi_n | \bar{\zeta} \rangle. \quad (7)$$

In addition, the time-dependent orbitals of Eqs. (5) and (6) are evaluated by a Trotter (split-operator) propagation,  $|\zeta(t \pm dt)\rangle = e^{\mp i H_0 dt} |\zeta(t)\rangle$ , for positive or negative times respectively.

#### D. Separable expression for $\langle \Sigma \rangle$

Given Eq. (2) and the separable form of Eq. (4) it immediately follows that

$$\langle \phi | \Sigma(t) | \phi \rangle \simeq \frac{1}{N_{\bar{\zeta}}} \sum_{\bar{\zeta}} \int \phi(\mathbf{r}) \zeta(\mathbf{r}, t) u(\mathbf{r}, t) d\mathbf{r}, \quad (8)$$

where

$$u(\mathbf{r}, t) = \int W(\mathbf{r}, \mathbf{r}', t) \bar{\zeta}(\mathbf{r}') \phi(\mathbf{r}') d\mathbf{r}'. \quad (9)$$

### IV. ACTING WITH THE RETARDED POLARIZATION POTENTIAL

To calculate  $u(\mathbf{r}, t)$  in Eq. (9), one needs to act with  $W(\mathbf{r}, \mathbf{r}', t)$  on the product  $\bar{\zeta}(\mathbf{r}') \phi(\mathbf{r}')$ . This will be done in two stages: First, we will calculate the action of the retarded (causal) effective-interaction:

$$u^R(\mathbf{r}, t) = \int W^R(\mathbf{r}, \mathbf{r}', t) \bar{\zeta}(\mathbf{r}') \phi(\mathbf{r}') d\mathbf{r}', \quad (10)$$

and the next section explains how to convert the causal  $u^R(\mathbf{r}, t)$  function to the time-ordered one  $u(\mathbf{r}, t)$ .

#### A. Deterministic $W^R$

It is well-known (Refs. 7 and 24) that linear-response TDH can be used to calculate the action of  $W^R$ . In our context, this amounts to perturbing all occupied states,

$$\phi_n^\lambda(\mathbf{r}, t=0) = e^{-i\lambda v_{\text{pert}}(\mathbf{r})} \phi_n(\mathbf{r}), \quad n \leq N_{\text{occ}}$$

where  $\lambda$  is small (typically  $10^{-4} E_h^{-1}$ ) and  $v_{\text{pert}}(\mathbf{r}) \equiv \int \nu(\mathbf{r}, \mathbf{r}') \bar{\zeta}(\mathbf{r}') \phi(\mathbf{r}') d\mathbf{r}'$ . Then one propagates simultaneously all occupied states,  $|\phi_n^\lambda(t+dt)\rangle = e^{-iH^\lambda(t)dt} |\phi_n^\lambda(t)\rangle$  using a time-dependent Hamiltonian:

$$H^\lambda(t) = H_0 + v_{\text{H}}^\lambda(\mathbf{r}, t) - v_{\text{H}}(\mathbf{r}), \quad (11)$$

where  $v_{\text{H}}^\lambda(\mathbf{r}, t) \equiv v_{\text{H}}[n^\lambda(t)](\mathbf{r})$ ,  $v_{\text{H}}(\mathbf{r}) \equiv v_{\text{H}}[n_0](\mathbf{r})$  and

$$n^\lambda(\mathbf{r}, t) = 2 \sum_{n \leq N_{\text{occ}}} |\phi_n^\lambda(\mathbf{r}, t)|^2,$$

where the density includes the spin factor. The causal response of Eq. (10) is then

$$u^R(\mathbf{r}, t) = \frac{v_{\text{H}}^\lambda(\mathbf{r}, t) - v_{\text{H}}(\mathbf{r})}{\lambda}. \quad (12)$$

An alternative to this RPA screening procedure is to replace the TDH by time-dependent DFT (TDDFT).[25] In principle, it is equivalent to the inclusion of a vertex function in  $W$ . [26, 27] Practical implementations with various approximate density functionals revealed that this approach is not universally successful [26, 28] but it often improves, at times dramatically, the energies of the unoccupied states.[19, 29]. Practically, the only required changes are the replacement of all the Hartree potentials in Eqs. (11) and (12) by the total Hartree-exchange-correlation part, e.g.,  $v_{\text{H}}^\lambda(\mathbf{r}, t) \rightarrow v_{\text{H}}^\lambda(\mathbf{r}, t) + v_{\text{xc}}[n^\lambda(t)](\mathbf{r})$ , etc.

As a second alternative, the RPA form used here could be followed by a zero-cost post processing self-consistency method, where a rigid shift is applied on the Green's function part. This method improves one-shot  $G_0W_0$  and brings it to agreement with experiment; see Ref. 30 for details.

#### B. Stochastic $W^R$

Deterministic linear-response TDH is expensive for large systems since all occupied states are propagated. We have therefore developed and applied a very cheap alternative, stochastic TDH.[19, 31, 32] For each  $|\bar{\zeta}\rangle$  one chooses and propagates a small set ( $N_\eta \sim 5 - 30$ ) of occupied stochastic functions formally defined as:

$$\eta_l(\mathbf{r}) = \sum_{n \leq N_{\text{occ}}} \eta_{nl} \phi_n(\mathbf{r}), \quad l = 1, \dots, N_\eta, \quad (13)$$

where the coefficients can be real or complex, and are either specified directly (e.g.,  $\eta_{nl} = \pm 1$ ) or based on a projection of a random vector  $\bar{\eta}_l(\mathbf{r})$ , i.e.,  $|\eta_l\rangle = P|\bar{\eta}_l\rangle$  (see Ref. 33). Then, completely analogously to the deterministic case, the stochastic-occupied states are perturbed

$$\eta_l^\lambda(\mathbf{r}, t=0) = e^{-i\lambda v_{\text{pert}}(\mathbf{r})} \eta_l(\mathbf{r}), \quad (14)$$

and propagated,

$$|\eta_l^\lambda(t+dt)\rangle = e^{-iH^\lambda(t)dt} |\eta_l^\lambda(t)\rangle, \quad (15)$$

and the time-dependent Hamiltonian is constructed again using Eq. (11) but now the Hartree potential  $v_{\text{H}}^\lambda(\mathbf{r}, t)$  is based on the density of the propagated stochastic-occupied orbitals,

$$n^\lambda(\mathbf{r}, t) = C_{\text{norm}} \frac{2}{N_\eta} \sum_{l \leq N_\eta} \eta_l^\lambda(\mathbf{r}, t)^2, \quad (16)$$

where  $C_{\text{norm}}$  is a normalization constant ensuring the correct total number of electrons ( $\int n^\lambda(\mathbf{r}, t) d\mathbf{r} = N_e$ ).

One last difference from the deterministic case is that it is necessary now to repeat the calculation with  $\lambda = 0$  and the response is then the difference of the time-dependent potentials

$$u^R(\mathbf{r}, t) = \frac{v_{\text{H}}^\lambda(\mathbf{r}, t) - v_{\text{H}}^{\lambda=0}(\mathbf{r}, t)}{\lambda}. \quad (17)$$

Note that this is not needed in the deterministic case where  $v_{\text{H}}^{\lambda=0}(\mathbf{r}, t) = v_{\text{H}}(\mathbf{r})$  does not change in time; but even without perturbation the stochastic TDDFT orbitals are not eigenstates and change in time leading to fluctuations in the density, so Eq. (17) is required to ensure that the response is indeed in the linear regime.

## V. FRACTURED STOCHASTIC ORBITALS AND THE CAUSAL TO TIME-ORDERED TRANSFORMATION

$W$  and  $W^R$  are related in Fourier space – they are the same for positive frequencies and are complex-conjugates at negative frequencies.[34] The same properties are true for  $u$  and  $u^R$ , as long as the source term ( $\zeta\phi$ ) in Eq. (10) is real. Practically, this gives a recipe for obtaining  $u$  from  $u^R$ , which we label as  $u = \mathcal{T}(u^R)$ , meaning: FFT  $u^R$  from time to frequency, conjugate at negative frequencies and inverse FFT the result back to time

$$\begin{aligned} u^R(\mathbf{r}, t) &\rightarrow u^R(\mathbf{r}, \omega) = \int_0^\infty e^{-\frac{1}{2}\gamma^2 t^2} e^{i\omega t} u^R(\mathbf{r}, t) dt \\ &\rightarrow u(\mathbf{r}, \omega) = \begin{cases} u^R(\mathbf{r}, \omega) & \omega \geq 0 \\ (u^R(\mathbf{r}, \omega))^* & \omega < 0 \end{cases} \quad (18) \\ &\rightarrow u(\mathbf{r}, t) = \frac{1}{2\pi} \int_{-\infty}^\infty e^{-i\omega t} u(\mathbf{r}, \omega) d\omega. \end{aligned}$$

This procedure is, however, storage intensive since the whole  $u^R(\mathbf{r}, t)$  from each core needs to be stored on disk.

### A. Stochastic basis

Our previous approach (Ref. 19) to solving the storage issue was based on a stochastic resolution of identity, Eq. (3),

$$u(\mathbf{r}, t) \simeq u_{\text{aprx}}(\mathbf{r}, t) \equiv \frac{1}{N_\xi} \sum \xi(\mathbf{r}) u_\xi(t), \quad (19)$$

where  $\xi(\mathbf{r}) = \pm (dV)^{-0.5}$  is a third set of random functions (beyond  $\zeta(\mathbf{r})$  and  $\eta(\mathbf{r})$ ). Here  $u_\xi(t)$  are obtained

by time-ordering ( $u_\xi = \mathcal{T}(u_\xi^R)$ ) the causal coefficients  $u_\xi^R(t) \equiv \lambda^{-1} (v_\xi^\lambda - v_\xi^{\lambda=0})$  where  $v_\xi^\lambda = \langle \xi | v_{\text{H}}^\lambda(t) \rangle$  (see Eq. (17)).

In the appendix, we prove that the relative error in the stochastic expansion of  $u$  (at a fixed time  $t$ ) is the ratio of the number of grid points and the number of stochastic vectors (cf., Eq. (A.5)):

$$\frac{\sigma^2(u(t))}{\langle u(t) | u(t) \rangle} \equiv \frac{\{ \langle u_{\text{aprx}}(t) - u(t) | u_{\text{aprx}}(t) - u(t) \rangle \}}{\langle u(t) | u(t) \rangle} = \frac{N_g}{N_\xi}.$$

This implies that the accuracy of the stochastic decreases with system size, unless  $N_\xi$  is increased. We previously (Refs. 19 and 20) used  $N_\xi = 100 - 300$ , but for the very large systems studied here  $N_\xi$  needs to be increased to avoid large statistical errors. For large  $N_\xi$ , however, the overlaps  $\langle \xi | u^R(t) \rangle$  dominate the computational cost, altering the linear scaling with system size.

### B. Fractured basis:

In order to overcome this drawback of the stochastic basis, we use random functions in Eq. (19) that are non-zero only over short segments rather than extending over the full grid; we label them as a “fractured” stochastic basis.

A simple example clarifies this concept. Break the  $N_g$  grid points to two sets  $A, B$ , each with  $N_g^A = N_g^B = \frac{1}{2} N_g$  points. Apply the stochastic resolution again with  $N_\xi$  functions, but now the first half of the functions ( $\xi_A$ ) are non-zero only over the  $A$ -set points, and the other half are non vanishing over the  $B$  set. Then, in an obvious notation:

$$u(\mathbf{r}, t) \simeq \begin{cases} \frac{1}{N_g^A} \sum_{\xi_A} \xi_A(\mathbf{r}) u_{\xi_A}(t) & \mathbf{r} \in A \\ \frac{1}{N_g^B} \sum_{\xi_B} \xi_B(\mathbf{r}) u_{\xi_B}(t) & \mathbf{r} \in B, \end{cases} \quad (20)$$

where  $u_{\xi_A}(t) \equiv \langle \xi_A | u \rangle_A \equiv dV \cdot \sum_{\mathbf{r} \in A} \xi_A(\mathbf{r}) u(\mathbf{r})$  and analogously for  $B$ .

The cost of calculating each  $u_{\xi_A}(t)$  is half that of calculating the original  $u_\xi(t)$ , since the summation includes half the grid points. But the squared standard deviation of  $u$  is unchanged!

$$\begin{aligned} \sigma^2(u) &= \sigma_A^2(u) + \sigma_B^2(u) = \\ &= \frac{N_g^A \langle u | u \rangle_A}{\frac{1}{2} N_\xi} + \frac{N_g^B \langle u | u \rangle_B}{\frac{1}{2} N_\xi} = \frac{N_g \langle u | u \rangle}{N_\xi}, \end{aligned}$$

where we used  $\langle u | u \rangle_A + \langle u | u \rangle_B = \langle u | u \rangle$ . This implies that the use of Eq. (19) instead of Eq. (20) reduces the numerical effort by a factor of two without affecting the statistical error.

Obviously, we could continue with this process of using smaller and smaller segments further. In practice, we

pick here a small segment size  $N_s \sim 0.001N_g - 0.01N_g$ , so that the ratio of total grid length and the segment length,  $L \equiv \frac{N_g}{N_s}$ , is  $\approx 1000$ . Each stochastic function now extends only over  $N_s$  points, so we label it as “fractured”. For simplicity, we do not even require the segments to be non-overlapping. The only requirement is to ensure that each point has the same  $L^{-1}$  probability to be sampled, i.e., to have a fractured basis function that includes it. [35]

The fractured-stochastic basis expansion is then:

$$u(\mathbf{r}, t) \simeq \frac{L}{N_\xi} \sum_{\xi \in \text{frac}} \xi(\mathbf{r}) u_\xi(t), \quad (21)$$

where the “frac” label indicates that the summation extends over fractured stochastic orbitals. Since each stochastic function  $\xi(\mathbf{r})$  is defined now only over  $N_s$  points, the total cost in the expansion is (for each time step) only  $N_s N_\xi$ , vs.  $N_g N_\xi$  in the original stochastic expansion (Eq. (19)). Therefore, a much larger  $N_\xi$  can now be used keeping the error in Eq. (21) in check.

We conclude this section by several observations:

1. The segments need to sufficiently sample each point; each grid point has a probability  $L^{-1}$  of being sampled by each of the  $N_\xi$  functions so it is important to have  $1 \ll L^{-1} N_\xi$ , i.e.,  $L \ll N_\xi$ . Put differently, the segment size cannot be too small.
2. One could rewrite Eq. (21) as a formal fractured-stochastic resolution of the identity, FS-RI:

$$\mathcal{I} \simeq \frac{L}{N_\xi} \sum_{\xi \in \text{frac}} |\xi\rangle \langle \xi|. \quad (22)$$

3. One could envision (although we have not done it here) that each segment would be non-contiguous, i.e., made from  $N_s$  random points from the full grid. We do not even have to ensure that the points in each segment are all different from each other, as long as they are randomly selected!

## VI. FINAL STOCHASTIC ALGORITHM

The final stochastic GW algorithm is therefore simple:

Choose  $N_{\bar{\zeta}} \sim 200 - 1000$  stochastic functions (the wall time is minimized if  $N_{\bar{\zeta}}$  CPU cores are used, i.e., one per  $\bar{\zeta}$ ). Then, for each choice of  $\bar{\zeta}$ :

1. Choose a set of  $N_\xi \sim 5,000 - 50,000$  fractured random functions  $\xi(\mathbf{r})$ , each with  $\frac{N_g}{L}$  grid points. Typically  $L \sim 100 - 1000$ .
2. Choose a set of  $N_\eta \sim 5 - 30$  stochastic-occupied functions  $\eta_l(\mathbf{r})$  (Eq. (13)).
3. Calculate  $v_{\text{pert}}(\mathbf{r})$  and perturb the  $\eta_l(\mathbf{r})$  per Eq. (14).

4. Propagate the perturbed  $\eta_l^\lambda(\mathbf{r}, t)$  per Eq. (15), calculating at each time step  $v_{\text{H}}^\lambda(\mathbf{r}, t)$  and constructing and storing in memory the set of  $v_\xi^\lambda(t)$ .
5. Repeat Step 4 for unperturbed functions (using  $\lambda = 0$ ), storing  $v_\xi^{\lambda=0}(t)$  along the propagation. Then at the end of the propagation calculate  $u_\xi^R(t)$  and apply a time-ordering operation  $u_\xi = \mathcal{T}(u_\xi^R)$  (analogous to Eq. (18)).
6. Then calculate  $\zeta(\mathbf{r}, t)$  for negative and positive times (Eqs. (5) and (6)) and use with Eq. (21) to accumulate the matrix element of the self-energy (Eqs. (8) and (9)).

Once steps 1-6 are finished average the resulting  $\langle \phi | \Sigma(t) | \phi \rangle$  from each core, Fourier transform the result and solve Eq. (1).

The algorithm above, using stochastic TDH, is the most efficient version for large systems. If deterministic TDH is used, the steps are similar except that instead of the stochastic occupied states  $\eta_l$  one perturbs and propagates the deterministic occupied states  $\phi_n(\mathbf{r})$  (and then there is no need to calculate  $v_\xi^{\lambda=0}(t)$ , which is obtained directly from the ground state density  $n(\mathbf{r})$ ).

## VII. SIMULATIONS AND RESULTS

The stochastic GW simulations were run on the Comet cluster with Intel Xeon E5-2680v3 processors (2.5 GHz clock speed). The implementation is trivially parallelized with speedup efficiency greater than 80% when using up to 1728 cores on 144 CPUs. In all calculations reported here all 12 cores on each CPU were used.

All simulations used uniform grids with isotropic spacing  $dx = dy = dz$ . For both molecules and periodic solids, the KS-LDA ground state was computed using Troullier-Martins pseudopotentials,[36] and a kinetic energy cutoff of  $28 E_h$ . For molecules, the Martyna-Tuckerman approach [37] was used to avoid the effect of periodic images.

### A. Finite systems

The new stochastic GW implementation was first tested on acenes with 1, 2, 4 and 6 rings as well as a  $C_{60}$  molecule. Table I lists the parameters used for each system. The uniform real-space grid spacing  $dx$  is sufficiently small to converge the LDA eigenvalues to  $< 10$  meV. Further, the QP shifts are generally less sensitive to  $dx$  than the LDA eigenvalues. The damping parameter  $\gamma$  cannot be too high to avoid over-broadening the features in  $\langle \phi | \Sigma(\omega) | \phi \rangle$ . For finite systems,  $\gamma = 0.1 E_h$  (cf., Eq. (18)) was sufficient to converge  $\varepsilon^{QP}$  (for a given  $N_{\bar{\zeta}}$ ) to better than 0.01 eV, although we used an even more conservative value of  $\gamma = 0.06 E_h$ .

System	$N_e$	$N_g$	$N_\eta$	HOMO	LUMO
Benzene	30	$(48)^3$	16	-9.18 $\pm$ 0.09	0.73 $\pm$ 0.09
Naphtalene	48	$48 \cdot 52 \cdot 60$	16	-8.12 $\pm$ 0.09	-0.60 $\pm$ 0.09
Tetracene	84	$48 \cdot 52 \cdot 82$	16	-6.82 $\pm$ 0.08	-1.80 $\pm$ 0.06
Hexacene	120	$48 \cdot 52 \cdot 104$	16	-6.18 $\pm$ 0.06	-2.42 $\pm$ 0.06
$C_{60}$	240	$(88)^3$	8	-7.80 $\pm$ 0.04	-3.27 $\pm$ 0.04
			16	-7.78 $\pm$ 0.04	-3.30 $\pm$ 0.04

Table I. Estimated QP energies (eV) for a set of finite systems with a fully stochastic approach. The calculations used  $dx = 0.35a_0$ ,  $N_{\bar{\zeta}} = 750$ ,  $N_{\xi} = 20000$ , and each fractured stochastic function extended over only  $L^{-1} = 1\%$  of the total grid.

To isolate the influence of the number of stochastic TDH functions,  $N_\eta$ , we studied the QP energies of the set of molecules with deterministic and stochastic TDH propagation (the latter with  $N_\eta = 16$ ). In both cases  $N_{\bar{\zeta}}$  was increased till the resulting statistical error for the HOMO and LUMO QP energies is  $\leq 0.05$  eV. Fig. 1 shows that the stochastic and deterministic calculations require similar  $N_{\bar{\zeta}}$ , so the residual statistical error due to the use of stochastic TDH is small.

The deterministic version scales quadratically with the size of the system so as shown in Fig. 1 it quickly becomes much more expensive than a constant- $N_\eta$  fully stochastic treatment. Beyond tetracene the CPU time of the fully stochastic approach (with a constant  $N_\eta$ ) scales linearly with a slope of less than 2 core-hours per electron.

Further, for large systems the number of propagated stochastic orbitals  $N_\eta$  can be reduced without increasing the stochastic error. This is illustrated for  $C_{60}$  where  $N_\eta = 8$  and  $N_\eta = 16$  (Table I) give an almost identical stochastic error.

## B. Periodic solids

We next studied the performance of stochastic  $GW$  for periodic systems employing large real space grids (equivalent to  $\Gamma$ -point sampling of large supercells in planewave codes). Specifically, we studied the scaling of stochastic  $GW$  for silicon and diamond supercells including several unit cells with lattice constants taken from experiment.[38, 39] The DFT eigenvalues were converged with respect to grid size to  $< 5$  meV, with grid spacings of around 0.45 and 0.35  $a_0$  in all directions for silicon and diamond, respectively. As in the molecular case, an energy-broadening parameter of  $\gamma = 0.06 E_h$  was sufficient for convergence.

Although the systems were large, most time was still spent on the TDH stage. The initial projection and preparation of the stochastic occupied orbitals,  $\bar{\zeta}(\mathbf{r})$  and  $\eta(\mathbf{r})$ , took at most 2% of the CPU time. In addition, the FS-RI stage (converting  $u^R$  to  $u$ , Sec. VB) took less than 5% of the total time when using  $L = 100$  (so each fractured orbital covers only 1% of the grid) and  $N_{\xi} = 20,000$ . With these parameters the component of

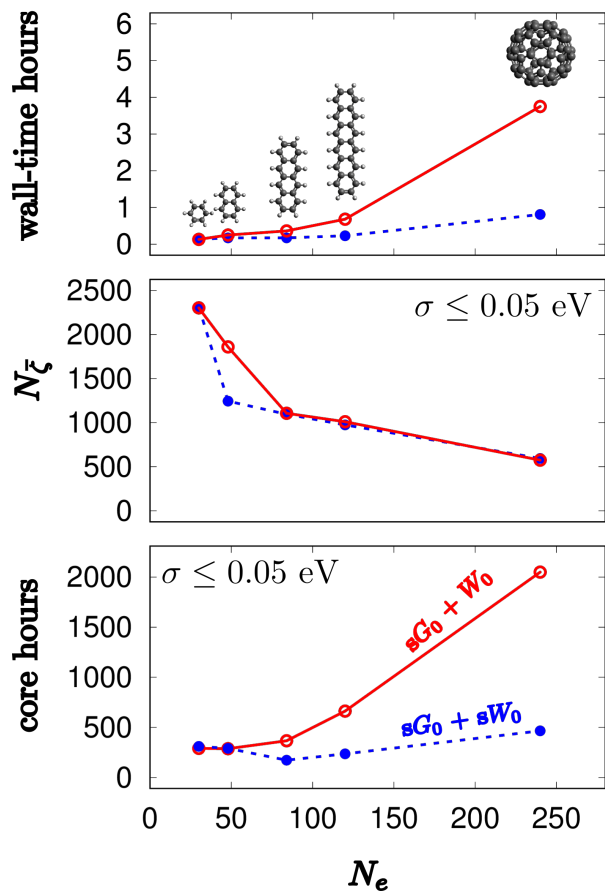


Figure 1. Resources needed to reduce the QP energy stochastic error to 0.05 eV for acenes and  $C_{60}$ . Top panel: Wall time (hours); the dashed and solid lines refer to deterministic and stochastic (with  $N_\eta = 16$ ) TDH propagations. Middle panel: Number of stochastic vectors  $N_{\bar{\zeta}}$ ; Bottom panel: required CPU core hours. All calculations used  $N_{\xi} = 20,000$  and  $L^{-1} = 1\%$ .

the stochastic error in the QP shifts due to the FS-RI is tiny, less than 0.01 eV.

We generally used  $N_\eta = 8$  propagated stochastic orbitals for periodic systems. Higher values do not change the predicted QP energies significantly, but reduce somewhat the statistical noise. When  $N_\eta = 16$  the fluctuations of  $E_g$  in a  $2 \times 2 \times 2$  supercell of diamond decrease by 8 (for the same  $N_{\bar{\zeta}}$ ). This is not sufficient to offset the cost (doubling the CPU time) of using  $N_\eta = 16$  so it is better to fix  $N_\eta = 8$  and use a larger  $N_{\bar{\zeta}}$ .

Table II, obtained with a fixed  $N_{\bar{\zeta}} = 400$ , shows that the stochastic error of  $E_g$  (the gap between the bottom of the conduction band and the top of the valance band) decreases rapidly with system size. Further, the number of stochastic vectors  $N_{\bar{\zeta}}$  required to decrease the error below 0.05 eV is plotted in Fig. 2. The lower panel shows that the total CPU time then scales at worst linearly with  $N_e$ . The initial slope (fitted to the four smallest systems) is 0.25 core hours per electron. The time to solution then quickly declines for larger supercells as the required  $N_{\bar{\zeta}}$

$N_{cells}$	$N_e$	$N_g$	$E_g$ (eV)			
			Diamond		Silicon	
8	256	$(42)^3$	5.36	$\pm 0.09$	1.17	$\pm 0.06$
27	864	$(60)^3$	5.28	$\pm 0.07$	1.35	$\pm 0.05$
64	2048	$(80)^3$	5.40	$\pm 0.06$	1.29	$\pm 0.04$
216	6912	$(120)^3$	5.55	$\pm 0.04$	1.24	$\pm 0.04$
343	10978	$(140)^3$	5.51	$\pm 0.04$	1.24	$\pm 0.03$

Table II. Estimated QP gaps for bulk carbon and silicon using  $N_{\bar{\zeta}} = 400$ ,  $N_{\eta} = 8$ ,  $N_{\xi} = 20,000$  and  $L = 100$ .  $N_{cells}$  is the number of conventional cells in a supercell,  $N_e$  the total number of valence electrons, and  $N_g$  is the total number of grid points.

decreases. For the largest supercells of both systems, we observe a linear slope of 0.06 core hours per electron. Specifically, calculations for diamond and silicon supercells with 10978 valence electrons consumed only about 1900 and 1000 core hours!

Per-electron the periodic calculations were much faster (up to almost 20 times!) than for finite systems. One obvious reason is that it is much easier to pack electrons in a periodic system, so, for example, the largest supercell of silicon or diamond has 50 times more electrons than  $C_{60}$  but its grid is only  $\sim 4$  times bigger. In addition, the large periodic systems have many more electrons so they required fewer samples ( $N_{\bar{\zeta}}$ ).

### VIII. DISCUSSION AND CONCLUSIONS

In conclusion, we introduced a general method for efficient stochastic sampling, fragmented stochastic resolution of the identity, (FS-RI). Here, we applied FS-RI to enhance our stochastic- $GW$  method. When combined with a simple direct projection approach to efficiently obtain random occupied orbitals from initial white noise vectors, the overall stochastic  $GW$  method is very fast, scales practically linearly, and makes it possible to calculate QP energies for systems with  $N_e > 10,000$  valence electrons in only a few thousands of CPU-core hours or less.

The overall algorithm is straightforward, and an open-source software (StochasticGW) is freely available.[40] Our calculations show very favorable scaling of the statistical error in all three types of stochastic samplings used in stochastic  $GW$ :

- FS-RI makes it possible to easily increase the number of number of such sampling vectors ( $N_{\xi}$ ) by 100-fold or more, from hundreds to tens of thousands. The key feature is that the accuracy is independent of the size of the fractured stochastic vectors as long as each grid point is sufficiently sampled (i.e., as long as  $L \ll N_{\xi}$ ). The FS-RI expansion (Eq. (21)) adds only a tiny stochastic error (less than 0.01 eV) and its cost is negligible.
- Very few propagated stochastic orbitals  $\eta$  are

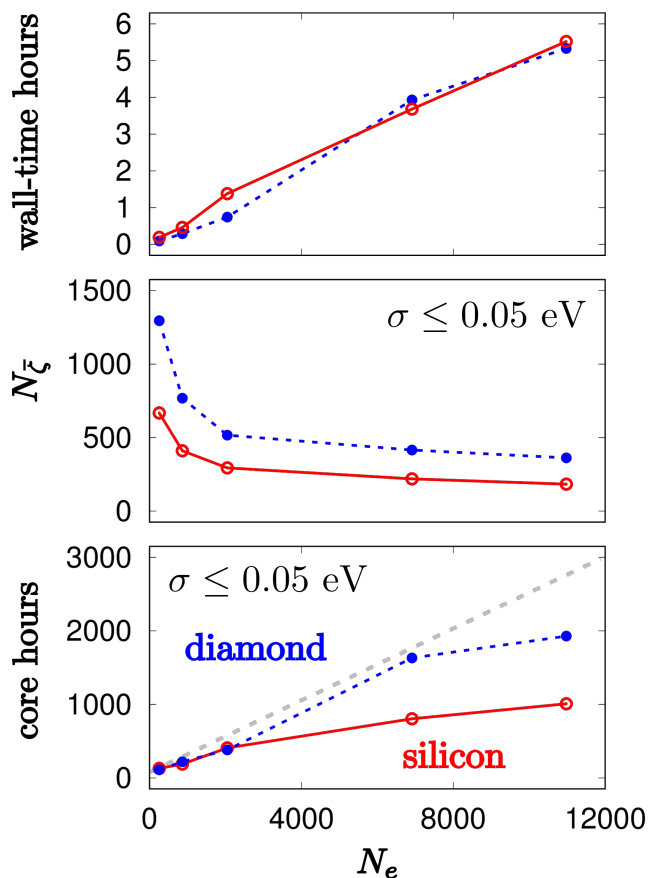


Figure 2. Resources required to lower the stochastic error in  $E_g$  to 0.05 eV for silicon and diamond supercells (red and blue, respectively). All calculations used  $N_{\eta} = 8$ ,  $N_{\xi} = 20,000$  and  $L^{-1} = 1\%$ . Top: CPU hours; Middle: Required  $N_{\bar{\zeta}}$ ; and bottom: Total CPU core hours.

needed for the TDH propagation – we used  $N_{\eta} = 16$  for molecules but even half that number,  $N_{\eta} = 8$ , was sufficient for large molecules and periodic solids.

- The stochastic error depends on the number of vectors used to sample the Green’s function,  $N_{\bar{\zeta}}$ . To obtain a low error of 0.05 eV in the quasiparticle energies,  $N_{\bar{\zeta}}$  is circa 1000 for small systems but decreases with system size so for  $C_{60}$  it is only 600 and for large periodic supercells it decreases to a few hundreds. Our calculations here and in Ref. [22] indicate that the stochastic fluctuations somewhat increases with  $E_g$ , but linear scaling is maintained.

Taken together, we find a very favorable scaling. Cells with 10978 valence electrons require less than 2000 core hours to yield QP energies with statistical errors below 0.05 eV. Our method thus makes it possible to calculate QP energies of extremely large systems with thousands of atoms on small computer clusters.

While our stochastic  $GW$  has a practically linear scaling wall-time, it has two ingredients which formally scale

non-linearly. We use occupied-projection, which scales as  $O(N_e^2)$ ; this by itself however is not a major issue since it will not be the dominant part of the calculation until we would reach  $N_e \gg 100,000$ . But more importantly, occupied-projection uses the occupied DFT eigenstates, and in most DFT codes the extraction of these states scales as  $O(N_e^3)$  and is prohibitive for very large systems. We therefore anticipate that when simulating systems with  $N_e > 50,000$  it may be necessary to switch back to Chebyshev-projection that avoids the eigenstates altogether, as long as the underlying DFT potential could be obtained by either linear scaling DFT [41–44] or stochastic DFT.[45, 46]

Finally, we note that the new technique invented in this paper, FS-RI, is potentially useful for a large number of applications that are unrelated to stochastic  $GW$ , including long-range exchange, stochastic MP2 (direct and exchange), and stochastic resolution of the identity.[33, 47, 48]

### ACKNOWLEDGMENTS

We are grateful for support by the Center for Computational Study of Excited State Phenomena in Energy Materials (C2SEP) at the Lawrence Berkeley National Laboratory, which is funded by the U.S. Department of Energy, Office of Science, Basic Energy Sciences, Materials Sciences and Engineering Division under contract No. DEAC02-05CH11231 as part of the Computational materials Sciences Program. V. V. greatly appreciates helpful discussion with Gabriel Kotliar and Mark Hybertsen. The calculations were performed as part of the XSEDE computational Project No. TG-CHE170058.[49]

### APPENDIX: STATISTICAL ERROR OF A STOCHASTIC BASIS EXPANSION

Given a stochastic expansion of a general function, analogous to Eq. (19),

$$|f\rangle \simeq |f_{\text{aprx}}\rangle \equiv \frac{1}{N_\xi} \sum |\xi\rangle \langle \xi|f\rangle, \quad (\text{A.1})$$

we show here that the average relative error in the representation of  $f$  is proportional to the number of grid points. Specifically, define

$$\begin{aligned} \sigma^2(f) &= \{\langle f_{\text{aprx}}|f_{\text{aprx}}\rangle\} - \langle f|f\rangle \\ &= \frac{1}{N_\xi^2} \left\{ \sum_{\xi, \xi'} \langle \xi|\xi'\rangle \langle f|\xi\rangle \langle \xi'|f\rangle \right\} - \langle f|f\rangle, \quad (\text{A.2}) \end{aligned}$$

where all functions are assumed real. Separating yields

$$\sigma^2(f) = J_1 + J_2 - \langle f|f\rangle. \quad (\text{A.3})$$

Here  $J_1$  is the  $\xi = \xi'$  contribution

$$\begin{aligned} J_1 &= \frac{1}{N_\xi^2} \left\{ \sum_{\xi'=\xi} \langle \xi|\xi\rangle \langle f|\xi\rangle \langle \xi|f\rangle \right\} \\ &= \frac{N_g}{N_\xi^2} \left\{ \sum_{\xi} \langle f|\xi\rangle \langle \xi|f\rangle \right\} = \frac{N_g}{N_\xi^2} \left\{ \sum_{\xi} \langle f|\xi\rangle \langle \xi|f\rangle \right\}, \end{aligned}$$

where the definition  $\xi(\mathbf{r}) = \pm(dV)^{-0.5}$  implies that  $\langle \xi|\xi\rangle = N_g$  (always, not just as an average). The resulting expression for  $J_1$  simply involves a resolution of the identity  $\{|\xi\rangle\langle \xi|\} = I$ , so

$$J_1 = \frac{N_g}{N_\xi^2} \sum_{\xi} \langle f|f\rangle = \frac{N_g}{N_\xi^2} N_\xi \langle f|f\rangle. \quad (\text{A.4})$$

Similarly,  $J_2$  is the  $\xi' \neq \xi$  contribution

$$J_2 = \frac{1}{N_\xi^2} \left\{ \sum_{\xi} \sum_{\xi' \neq \xi} \langle \xi|\xi'\rangle \langle \xi'|f\rangle \langle f|\xi\rangle \right\},$$

and since the condition  $\xi' \neq \xi$  does not restrict  $\xi'$ , the resolution of the identity  $I = \{|\xi'\rangle\langle \xi'|\}$  is still valid, so

$$\begin{aligned} J_2 &= \frac{1}{N_\xi^2} \left\{ \sum_{\xi} \sum_{\xi' \neq \xi} \langle \xi|f\rangle \langle f|\xi'\rangle \right\} \\ &= \frac{1}{N_\xi^2} \sum_{\xi} \sum_{\xi' \neq \xi} \langle f|f\rangle = \frac{\langle f|f\rangle}{N_\xi^2} N_\xi (N_\xi - 1). \end{aligned}$$

Adding the terms gives

$$\frac{\sigma^2(f)}{\langle f|f\rangle} = \frac{(N_g - 1)}{N_\xi} \simeq \frac{N_g}{N_\xi}, \quad (\text{A.5})$$

as stipulated.



- 
- [1] P. Hohenberg and W. Kohn, Phys. Rev. **136**, 864 (1964).
- [2] R. M. Dreizler and E. K. U. Gross, *Density Functional Theory: An Approach to the Quantum Many-Body Problem* (Springer Science & Business Media, 1990).
- [3] R. M. Martin, *Electronic Structure: Basic Theory and Practical Methods* (Cambridge University Press, 2004) p. 624.
- [4] F. Aryasetiawan and O. Gunnarsson, Reports Prog. Phys. **61**, 237 (1998).
- [5] I. Shavitt, Mol. Phys. **94**, 3 (1998).
- [6] C. D. Sherrill and H. F. Schaefer III, in *Advances in quantum chemistry*, Vol. 34 (Elsevier, 1999) pp. 143–269.
- [7] R. M. Martin, L. Reining, and D. M. Ceperley, *Interacting Electrons* (Cambridge University Press, 2016).
- [8] D. Rowe, Rev. Mod. Phys. **40**, 153 (1968).
- [9] J. F. Stanton and R. J. Bartlett, J. Chem. Phys. **98**, 7029 (1993).
- [10] A. I. Krylov, Annu. Rev. Phys. Chem. **59** (2008).
- [11] L. Hedin, Phys. Rev. **139**, A796 (1965).
- [12] M. S. Hybertsen and S. G. Louie, Phys. Rev. B **34**, 5390 (1986).
- [13] P. Umari, G. Stenuit, and S. Baroni, Phys. Rev. B **79**, 201104 (2009).
- [14] P. Umari, G. Stenuit, and S. Baroni, Phys. Rev. B **81**, 115104 (2010).
- [15] J. Deslippe, G. Samsonidze, D. A. Strubbe, M. Jain, M. L. Cohen, and S. G. Louie, Comput. Phys. Commun. **183**, 1269 (2012).
- [16] M. P. Ljungberg, P. Koval, F. Ferrari, D. Foerster, and D. Sanchez-Portal, Phys. Rev. B **92**, 075422 (2015).
- [17] M. Govoni and G. Galli, J. Chem. Theory Comput. **11**, 2680 (2015).
- [18] J. Wilhelm, D. Golze, L. Talirz, J. Hutter, and C. A. Pignedoli, The journal of physical chemistry letters **9**, 306 (2018).
- [19] D. Neuhauser, Y. Gao, C. Arntsen, C. Karshenas, E. Rabani, and R. Baer, Phys. Rev. Lett. **113**, 076402 (2014).
- [20] V. Vlček, E. Rabani, D. Neuhauser, and R. Baer, J. Chem. Theory Comput. **13**, 4997 (2017).
- [21] V. Vlček, H. R. Eisenberg, G. Steinle-Neumann, D. Neuhauser, E. Rabani, and R. Baer, Phys. Rev. Lett. **116**, 186401 (2016).
- [22] V. Vlček, E. Rabani, and D. Neuhauser, Phys Rev Mater **2**, 030801 (2018).
- [23] Note that generally quantities in time and frequency use the same symbol, and the specifics are clear from the argument.
- [24] L. Hedin, Journal of Physics: Condensed Matter **11**, R489 (1999).
- [25] E. Runge and E. K. Gross, Phys. Rev. Lett. **52**, 997 (1984).
- [26] R. Del Sole, L. Reining, and R. Godby, Phys. Rev. B **49**, 8024 (1994).
- [27] F. Bruneval, F. Sottile, V. Olevano, R. Del Sole, and L. Reining, Phys. Rev. Lett. **94**, 186402 (2005).
- [28] A. Grüneis, G. Kresse, Y. Hinuma, and F. Oba, Phys. Rev. Lett. **112**, 096401 (2014).
- [29] L. Hung, F. H. da Jornada, J. Souto-Casares, J. R. Chelikowsky, S. G. Louie, and S. Ögüt, Phys. Rev. B **94**, 085125 (2016).
- [30] V. Vlček, R. Baer, E. Rabani, and D. Neuhauser, arXiv preprint arXiv:1701.02023 (2017).
- [31] Y. Gao, D. Neuhauser, R. Baer, and E. Rabani, J. Chem. Phys. **142**, 034106 (2015).
- [32] E. Rabani, D. Neuhauser, and R. Baer, Phys. Rev. B **91**, 235302 (2015).
- [33] D. Neuhauser, E. Rabani, Y. Cytter, and R. Baer, J. Phys. Chem. A **120**, 3071 (2015).
- [34] A. L. Fetter and J. D. Walecka, *Quantum Theory of Many Particle Systems* (McGraw-Hill, New York, 1971) p. 299.
- [35] If a segment starting point is chosen near the first or last point in the grid, then either the function should be wrapped (so a portion of the segment is near the end of the grid and another portion is near the beginning of the grid) or it should be padded (at the beginning or end) with zeros, to guarantee that all points are equally sampled.
- [36] N. Troullier and J. L. Martins, Phys. Rev. B **43**, 1993 (1991).
- [37] G. J. Martyna and M. E. Tuckerman, J. Chem. Phys. **110**, 2810 (1999).
- [38] T. Yamanaka and S. Morimoto, Acta Crystallogr., Sect. B: Struct. Sci **52**, 232 (1996).
- [39] A. D. Elliot, Acta Crystallogr., Sect. B: Struct. Sci **66**, 271 (2010).
- [40] The StochasticGW code is available under GPL at <http://www.stochasticgw.com>.
- [41] W. Yang, Physical Review Letters **66**, 1438 (1991).
- [42] E. Hernández and M. Gillan, Physical Review B **51**, 10157 (1995).
- [43] S. Mohr, L. E. Ratcliff, L. Genovese, D. Caliste, P. Boulanger, S. Goedecker, and T. Deutsch, Physical Chemistry Chemical Physics **17**, 31360 (2015).
- [44] J. VandeVondele, U. Borstnik, and J. Hutter, Journal of chemical theory and computation **8**, 3565 (2012).
- [45] R. Baer, D. Neuhauser, and E. Rabani, Phys. Rev. Lett. **111**, 106402 (2013).
- [46] D. Neuhauser, R. Baer, and E. Rabani, J. Chem. Phys. **141**, 041102 (2014).
- [47] D. Neuhauser, R. Baer, and D. Zgid, J. Chem. Theory Comput. **13**, 5396 (2017).
- [48] T. Y. Takeshita, W. A. de Jong, D. Neuhauser, R. Baer, and E. Rabani, J. Chem. Theory Comput. **13**, 4605 (2017).
- [49] J. Towns, T. Cockerill, M. Dahan, I. Foster, K. Gaither, A. Grimshaw, V. Hazlewood, S. Lathrop, D. Lifka, G. D. Peterson, *et al.*, Computing in Science & Engineering **16**, 62 (2014).